

Fault Location in VSC-HVDC Systems Based on NSGA-II and Discrete Wavelet Transform

Reza Rohani * , Amangaldi Koochaki *[‡] , Jafar Siahbalaee * 

*Department of Electrical Engineering, Aliabad Katoul Branch, Islamic Azad University, Aliabad Katoul, Iran

(Reza.Rohani@iau.ac.ir, koochaki@aliabadiu.ac.ir, j.siahbalaee@aliabadiu.ac.ir)

[‡]Corresponding Author; Amangaldi Koochaki, Department of Electrical Engineering, Aliabad Katoul Branch, Islamic Azad University, Aliabad Katoul, Iran, Tel: +98 1734239511,

Fax: +98 1733236473, koochaki@aliabadiu.ac.ir

Received: 08.05.2022 Accepted: 20.06.2022

Abstract- This paper introduces a novel fault location model based on Adaptive Neuro-Fuzzy Inference System (ANFIS). For the purpose of performance improvement, a meta-heuristic algorithm known as Non-Dominated Sorting Genetic Algorithm type 2 (NSGA-II), which has the ability of fast searching for the optimal point and escaping the local optimality trap, is used for ANFIS training. The fault current and voltage are usually the two parameters used as the inputs to the ANFIS, even though they cannot truly specify the fault characteristics on their own. Here, Discrete Wavelet transform (DWT) is used to extract the relevant features of the fault current. To demonstrate superiority of the proposed model, a comparative study is performed against the traditional Least-Squares and Back-Propagation (LS+BP) and Chaotic Dynamic Weight Particle Swarm Optimization (CDW-PSO) methods. The simulation results show that the proposed estimation model has a superior performance compared to the previous models in terms of both convergence speed and estimation error.

Keywords Fault location estimation, VSC-HVDC system, Adaptive neuro-fuzzy inference system, Non-dominated sorting genetic algorithm II, Discrete wavelet transform

1. Introduction

The High Voltage Direct Current (HVDC) transmission system is an effective large scale power transmission method with minimum power loss, especially over long distances [1], which has progressed considerably with the progress of power electronics and usage of high power switches in DC-AC and AC-DC converters [2]-[5]. Application of VSC-HVDC system brings many advantages, however the HVDC systems are subject to various faults that, if not detected in time, will impose heavy losses on network equipment [6]. Consequently, a good deal of studies have been carried out to estimate the locations of faults in these systems, e.g. differential protection techniques [7] which is costly method. Thus, numerous fault location models have been proposed in the papers to pave the way to overcome the problem ahead [8]. Two conventional methods for fault location in power systems are neural network [9] - [13], and Travelling-Wave (TW) [14] - [17]. These methods have a major drawback that

is requirement of the reflected wave speed and arrival time of the wave-front for fault location estimation, which are difficult to measure. To cope this challenge, feature extraction methods have been introduced like Singular Value Decomposition (SVD) [18] - [19], Fast Fourier Transform (FFT) [20], Hilbert Huang Transform (HHT) [21] - [23] and Wavelet Transform (WT) [24] - [25]. The extracted features obtained by these methods will then be applied to an estimator model. A number of estimation models have been proposed in the articles, for instant Support Vector Machine (SVM) [26] - [27], Extreme Learning Machine (ELM) [28], Random Forest (RF) [29] - [30], Gaussian Process Regression (GPR) [31], and Artificial Neural Network (ANN) [32],[33]. The majority of the estimation methods are based on machine learning techniques, wherein the SVM and ANN have the most applications [34]. Unlike ANN, SVM-based techniques do not depend on the number of features. This characteristic is especially important in fault detection and localization since required features can be extracted

directly from the original data without further need for pre-processing [35]. The SVM is a computational learning technique that performs estimation based on the statistics received from feature extraction models [36]. It has more success in classification and regression analysis applications; however, due to its high computational cost and lack of probable estimations, it is not very accurate in applications which involves in estimating parameter with uncertainty [37]. In contrast, Adaptive Neuro-Fuzzy Inference System (ANFIS) is a successful estimation technique being widely used in studies related to classification and fault location estimation within the different areas of the power system [38] - [41]. The classic structure of ANFIS has three fundamental limitations: (1) it depends on the type and number of membership functions, (2) the optimal location of the membership functions must be specified, and (3) limitations with respect to dimensions [42]. As a remedy to these problems, ANFIS has been used along with feature extraction techniques to alleviate the input dimensions, while intelligent algorithms are applied to optimize its parameters.

One of the commonly used feature extraction schemes is discrete wavelet transform (DWT), where the output can be extracted as approximate and detailed coefficients [43]. In order to train ANFIS and calculate its optimal parameters, the traditional least squares and back-propagation (LS+BP) method is used; this has, however, poor performance in terms of convergence speed and estimation error [44]. To enhance the performance of the ANFIS, various optimization algorithms can be used to train this system. The main benefit of the optimal training of the ANFIS using meta-heuristic optimization algorithms is prediction or estimation error reduction and fast convergence, particularly in real-time estimation applications. Numerous novel optimization algorithms with fantastic features are proposed in the literature. In [45], a novel modified Whale optimization algorithm is utilized for congestion control in power systems. In this algorithm, the coordination between the exploration and exploitation processes is modified by introducing two correction factors that prevent the algorithm from premature convergence. Similar studies are presented in [46] and [47] using modified Grey Wolf and Moth Flame optimization algorithms, respectively. A congestion management scheme is proposed in [48]. The real power delivery of the generators is optimally rescheduled using the Elephant Herd optimization algorithm to minimize the congestion cost. The congestion management (CM) problem in a deregulated power system environment in the presence of wind farms is solved in [49] by utilizing the Gravitational Search Algorithm (GSA). The most sensitive generators are sorted for participating in the CM problem according to the minimization of the active power yield of each generator.

Inspired by the biological models of living organisms, the Non-dominated Sorting Genetic Algorithm type 2 (NSGA-II) is a novel meta-heuristic algorithm with significant characteristics. In this algorithm, the reproduction characteristics of organisms are modeled as an objective function; over time, by applying the mutation and crossover operators on the previous generation, the next generation is

formed, which is better than the previous generation in terms of reproduction characteristics [50]. High-speed convergence and escaping from the local optimal traps are the unique features of this algorithm [51] - [52].

In this paper, the Daubechies-2 (db-2) mother wavelet has been used and 6 levels (1 approximate and 5 detailed levels) are formed for each fault signal. Finally, the set of the extracted features is applied to ANFIS for training and testing purposes. In order to improve performance of ANFIS, the NSGA-II algorithm is utilized; then, performance of the estimation model is compared with the default ANFIS-LS + BP model in terms of convergence speed and estimation error. In the previous study, the Chaotic Dynamic Weight Particle Swarm Optimization (CDWPSO) algorithm was used to optimize the ANFIS parameters [53]. To compare the performance of the proposed ANFIS-NSGA-II + DWT estimation model, in this study, CDWPSO, PSO and GA algorithms will also be considered for ANFIS training and the results will subsequently be compared with the proposed estimation model.

The performance of the NSGA-II optimization algorithm is already confirmed in [54] for multi-objective flexible workshop scheduling. The main advantage of this algorithm is its capability to handle multi-objective problems. However, the selection operation factor of the NSGA-II differs from the traditional GA. In this phase of optimization, the fitness function is calculated according to the domination of the initial population, so the distribution characteristics of the Pareto optimal solution set could be ensured. In addition, the population diversity is guaranteed by extending the individuals in the quasi-Pareto domain to the whole Pareto domain with uniform distribution. This will improve the convergence speed and stability of the optimization algorithm.

The novelty of the paper can be summarized as follows:

- Using the discrete wavelet transform scheme with 9 features extracted from the fault current signal, which have been explained in [55] - [56]. It is confirmed that there are various features that can be extracted from the fault signal according to the DWT scheme; however, to the best knowledge of the authors, these 9 statistical features have never been used in the literature related to the power system applications.
- In order to evaluate the performance of the training algorithm, i.e. NSGA-II, a comparative study using some conventional optimization methods including LS + BP, PSO, GA and CDWPSO are performed in terms of their convergence speed and estimation error
- The DWT-based feature extraction methods typically apply a vector of extracted features to machine learning algorithms [43]. In this paper, 6 levels consisted of approximate and detailed coefficients are extracted, where each level is comprised of 9 extracted features for 24 different fault intervals. Therefore, for each level, a feature matrix will be obtained that improves the estimation accuracy.

The article proceeds as follows. In section two, the proposed estimation model consisting of the Adaptive Neuro-Fuzzy Inference System, the DWT based feature extraction model, and the NSGA-II optimization algorithms explained. In section three, the VSC-HVDC system under study is presented and various faults are simulated to generate the initial inputs. Next, the features, supposedly being the inputs to ANFIS, will be extracted by DWT method. The performance results of the proposed ANFIS-NSGA-II + DWT estimation model are presented and furthermore compared with other estimation models at the end of this section. Finally, section four will summarize and conclude the paper.

2. Proposed Estimation Model

The structure of the proposed ANFIS-based fault location estimation model is shown in Fig. 1. From this figure, the estimation model is consisted of three main blocks: the first block illustrates the VSC-HVDC system under study; the second block shows the feature extraction technique, wherein the effective features are extracted from the fault current signal and subsequently fed into the estimator; and the third block is an ANFIS-based estimator that pinpoints the fault location in the HVDC system based upon the features provided by the second block. For the purpose of training the ANFIS, in this paper, the Non-dominant Sorting Genetic Algorithm Type 2 has been adopted. To extract the effective features of the fault current signal with a sampling rate of 10-3 seconds will be fed as input into the ANFIS. Also, the traditional LS + BP method will be implemented separately for the ANFIS training and the results will be compared with those of the NSGA-II algorithm in terms of estimation error and convergence speed. To demonstrate the superior performance of the proposed estimation model, a similar scenario will also be run with the classic CDWPSO, PSO and GA as the training algorithms of ANFIS and the result will be compared against those of the proposed model.

In the VSC-HVDC system under study, based on the location of fault, two types of faults are defined: internal and external. In Fig. 2, different fault zones are illustrated for the VSC-HVDC system. It should be noted that since the fault measurement is conducted on the M side, when a fault occurs in section hj it would be considered as an external fault, while an occurrence of fault in section jk will be identified as internal. To discern the internal and external faults, the Variance Contribution Rate (VCR) criterion has been adopted [57]. This criterion reflects the effects of amplitude and frequency fluctuations on the characteristics of the main signal at different scales. By definition, VCR_k for the kth distance would be:

$$VCR_k = \frac{\text{var}(c_i(t))}{\sum_{k=1}^L (\text{var}(c_{i_k}(t)) + \text{var}(r_{i_k}(t)))} \times 100 \quad (1)$$

in which, L is number of divisions on the transmission line, c_{ik}(t), the approximate coefficient for the kth division and r_{ik}(t), the final remainder of the difference between the original signal and the corresponding approximate version derived by DWT technique for each distance k:

$$r_i(t) = x_i(t) - p_i(t) \quad (2)$$

here, x_i(t) is the original fault current signal and p_i(t), the approximate version derived by DWT.

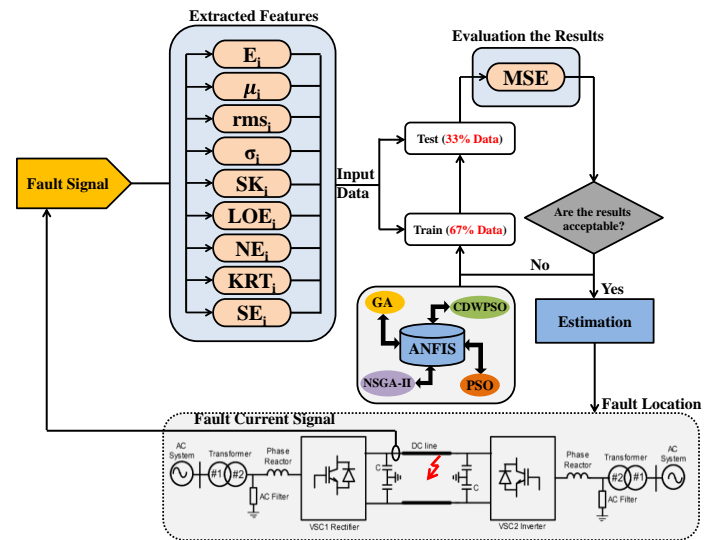


Fig. 1. The schematic structure of the proposed fault location estimator

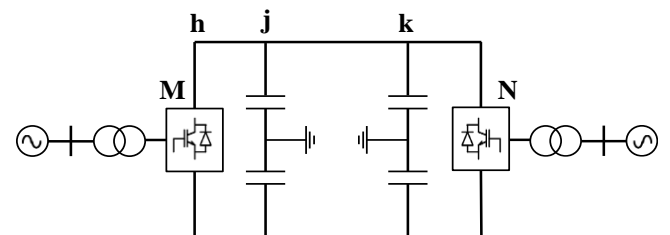


Fig. 2. Fault zones in the two-terminal VSC-HVDC system

2.1 Adaptive Neuro-Fuzzy Inference System(ANFIS):

Fig. 3 illustrates the structure of a two-input ANFIS [52]. The traditional LS+BP algorithm has been used for training and parameter adjustment. In ANFIS, there are two parameters known as Antecedent and Conclusion. The logical dependency between the inputs and output will be formed by adjusting these parameters [58].

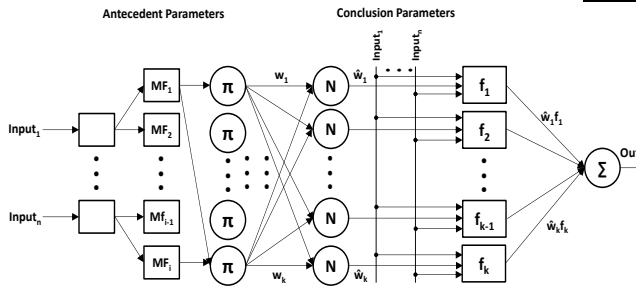


Fig. 3. ANFIS configuration

2.2 Non-dominant Sorting Genetic Algorithm Type 2 (NSGA-II):

The NSGA-II algorithm is a form of multi-objective GA algorithms with unique properties with respect to convergence and optimization response. The steps of this algorithm can be summarized as Algorithm 1 [59]:

Algorithm 1: Pseudo code of NSGA-II

- 1- Initialize population
- 2- Evaluate objective or fitness function
- 3- Assign rank to each individual based on Pareto Dominance
- 4- Calculate the Crowding Distance (CD)
- 5- Combine the initial population with the new individuals (new individuals or offspring which are produced by mutation and crossover processes)
- 6- Replace parents with the best individuals from the combined new population. To this end, in the first stage, those individuals whose fitness functions are found to be lower, through ranking, will be replaced by the previous parents and the new population will be sorted based on their crowding distance (CD). The initial population and the population resulted from the application of the mutation and crossover operators would be sorted during this stage, and those with lower fitness functions would be eliminated afterwards. In the next stage, the remaining population will be sorted again according to their crowding distance.
- 7- Repeat this process until stopping condition of the algorithm is met. The stopping condition is determined either by the limitation on the number of iterations of the algorithm or by the fitness function quality condition.
- 8- It must be noted that the crowding distance factor is a parameter used to select the solutions from the front of the possible solutions. The following assumptions are made on the CD:
 - The crowding distance between the first and last points of the front of possible solutions is infinite.
 - For any given point from the front of possible solutions, the crowding distance is calculated

$$\text{according to: } CD[i] = \frac{f_m^{i+1} - f_m^{i-1}}{f_m^{\max} - f_m^{\min}}$$

- where, $CD[i]$ is the crowding distance of the i^{th} individual over the front of possible solutions, i.e., F ; f_m^i is the m^{th} fitness function for the i^{th} individual over the front F ; and f_m^{\min} and f_m^{\max} are, respectively, the minimum and maximum values of the m^{th} fitness function over the front F . Among the possible solutions of the front, the one with the highest CD will be chosen as the optimal solution

2.3 Discrete Wavelet Transform

The discrete wavelet transform has been used in this study to extract the useful features by applying in the fault signal. Feature extraction is a method of data pre-processing which takes a pattern of data and extracts a series of useful features from it. High accuracy and low computational time are the main characteristics of this method [60]. In this method, the main signal $xi(t)$ is decomposed into a series of detailed and approximate components, i.e. wavelet coefficients that are indicated by ci . In order to apply DWT, the db-2 parent wavelet will be used throughout the paper [61]. Since, here, signal variations and sampling rate of the fault current signal are supposedly high, the db-2 parent wavelet will be used [62]. By defining 6 levels of resolution in DWT, 1 approximate level and 5 detailed levels will be obtained. In this paper, the fault current signal is considered as the main signal and measured on the M side; for each level, 9 DWT features are extracted [56], [60]. These features are Energy (E_i), Shannon Entropy (SE_i), Log Energy Entropy (LOE_i), Norm Entropy (NE_i), Root Mean Square (rms_i), Mean Value (μ_i), Standard Deviation (σ_i), Skewness (SK_i), and Kurtosis (KRT_i) which are calculated according to the eqs. (4) – (12), respectively. A simple structure of the feature extraction scheme based on DWT is depicted in Fig. 4.

$$E_i = \sum_{j=1}^N |c_{ij}|^2 \tag{4}$$

$$SE_i = - \sum_{j=1}^N c_{ij}^2 \log(c_{ij}^2) \tag{5}$$

$$LOE_i = \sum_{j=1}^N \log(c_{ij}^2) \tag{6}$$

$$NE_i = \sum_{j=1}^N c_{ij}^P \quad P \geq 1 \tag{7}$$

$$rms_i = \sqrt{\frac{1}{N} \sum_{j=1}^N c_{ij}^2} \tag{8}$$

$$\mu_i = \frac{1}{N} \sum_{j=1}^N c_{ij} \tag{9}$$

$$\sigma_i = \left(\frac{1}{N} \sum_{j=1}^N (c_{ij} - \mu_i)^2 \right)^{\frac{1}{2}} \tag{10}$$

$$SK_i = \sqrt{\frac{1}{6N} \sum_{j=1}^N \left(\frac{c_{ij} - \mu_i}{\sigma_i} \right)^3} \tag{11}$$

$$KRT_i = \sqrt{\frac{N}{24} \left(\frac{1}{N} \sum_{j=1}^N \left(\frac{c_{ij} - \mu_i}{\sigma_i} \right)^4 - 3 \right)} \tag{12}$$

In eqs. (4) - (12), c_{ij} is the combination of the detailed and approximate coefficients corresponding to the i th level .

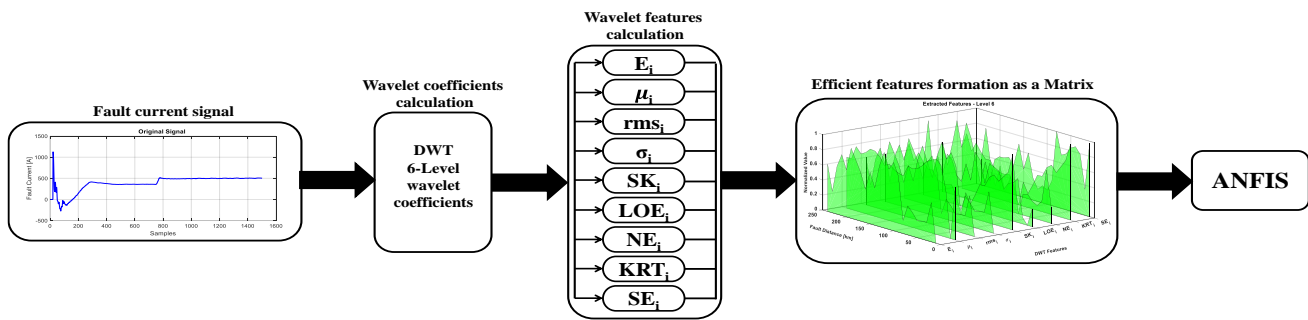


Fig. 4. Simple structure of the DWT-based feature extraction scheme

Measurement of the fault current signal for the internal Pole-To-Ground (PTG) fault has been carried out at distance intervals of 10 km [10 km - 240 km]; for each signal, 9 DWT features are calculated. To compare and display the extracted features better, all values are normalized according to eq.(13) for displaying in the range of [0 1] [53].

$$f_{norm} = \frac{f - f_{min}}{f_{max} - f_{min}} \tag{13}$$

After extracting the effective features and applying them to ANFIS, out of the total 1296 extracted features, 500 will be used for ANFIS training and the rest for its testing. In order to train ANFIS and determine the antecedent and conclusion parameters, the traditional LS + BP method and

the proposed NSGA-II algorithm will be used. In this paper, the Mean Squared Error (MSE) is assumed as the objective function according to eq. (14) [53]:

$$MSE = \frac{1}{N} \sum_{j=1}^N |A_j - E_j|^2 \tag{14}$$

in which, A_j is the actual output value of the j th training sample and E_j , the estimated value provided ANFIS for the j th training sample. Also, N denotes the size of training samples. Finally, the flowchart of the proposed fault location estimator can be illustrated as Fig.5. Also, Figs. 6-11 show the extracted features versus the fault distance for the 6 resolution levels.

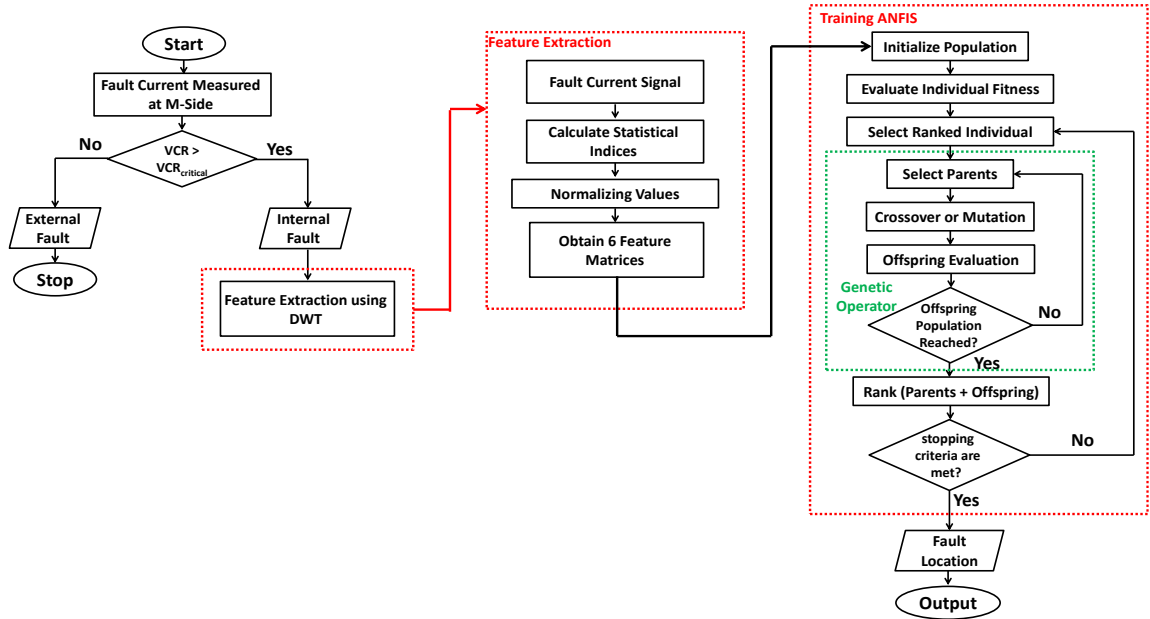


Fig. 5. Flowchart of the proposed fault location estimator

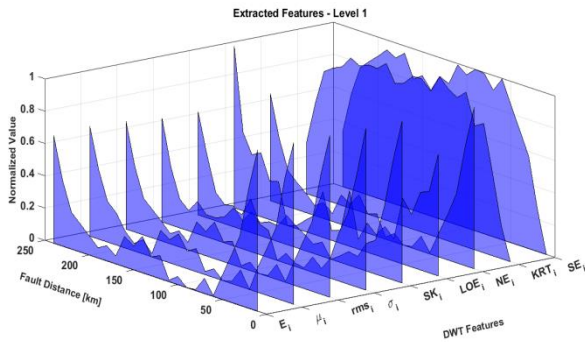


Fig.6. The DWT-based extracted features - level 1

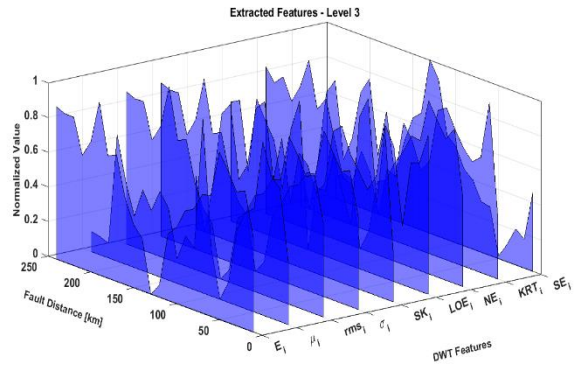


Fig.8. The DWT-based extracted features - level 3

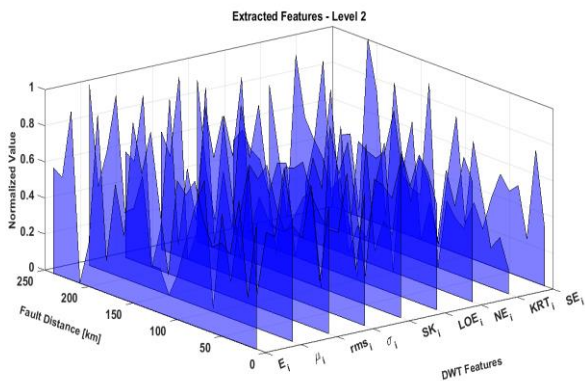


Fig.7. The DWT-based extracted features - level 2

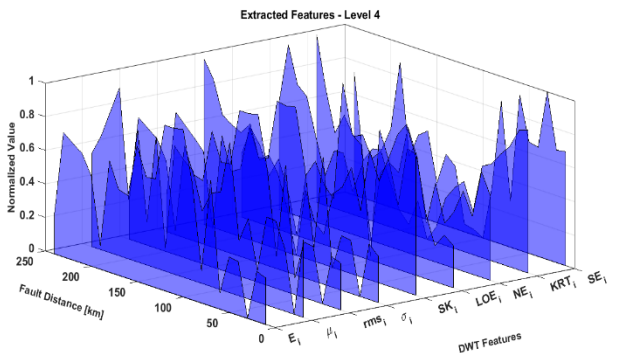


Fig. 9. The DWT-based extracted features - level 4

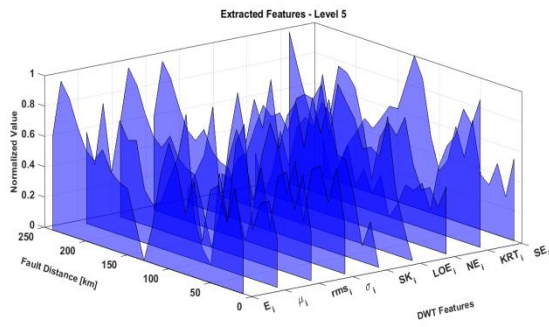


Fig.10. The DWT-based extracted features - level 5

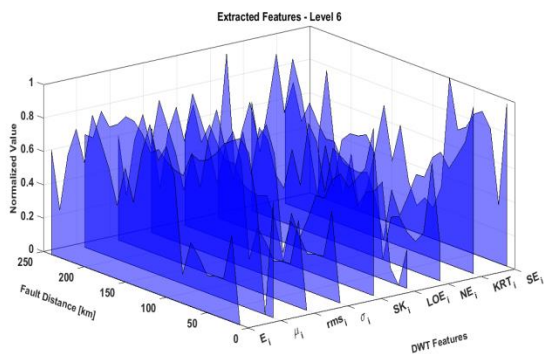


Fig. 11.The DWT-based extracted features - level 6

3. Simulation Results

In this paper, a 250 km two-terminal VSC-HVDC system with a nominal transmission voltage of 230 kV and an apparent power of 2000 MVA has been implemented in MATLAB/Simulink software environment, and PTG faults are simulated at 10 km distance intervals with a fault resistance of 100 Ω, as can be seen in Fig. 12. Since the simulation has been performed for a duration of 1.5 seconds while the sampling rate is 10-3 seconds, 1500 samples will be obtained for the fault current signal of each case. The PTG fault current signal at [0.75 s 1.5 s] and 10 km from the point M, is plotted in Fig.13. Also, the approximate and detailed coefficients related to the 6 resolution levels, resulted from applying DWT, can be seen in Fig.14. In this method, for each fault current signal, 1 approximate version and 5 detailed versions have been derived. From the difference between the approximate version and the original signal, the remainder r_i will be obtained using eq.(2). According to (1), for each fault signal at the k th distance, a VCR value can be obtained. Fig.15 shows variations of VCR criterion versus fault distance. To distinguish between the external and internal faults, a threshold value is defined for VCR, herein, $VCR_{critical} = 1\%$ has been chosen [57]. According to the

flowchart of Fig.5, to determine if the fault is external or internal, the VCR value will be compared to the threshold value. For external faults occurring within the h_j zone in Fig. 2, a VCR value less than 1% is obtained, while the VCR values for internal faults within the jk zone would be large.

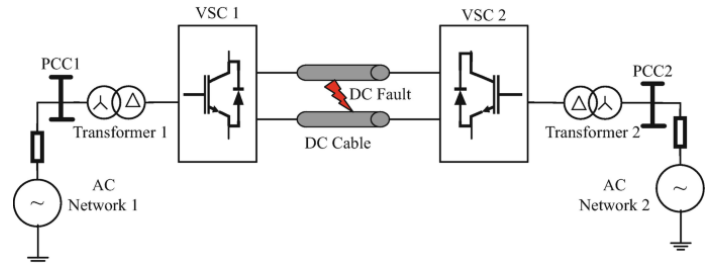


Fig. 12. The faulty two-terminal VSC-HVDC system under study

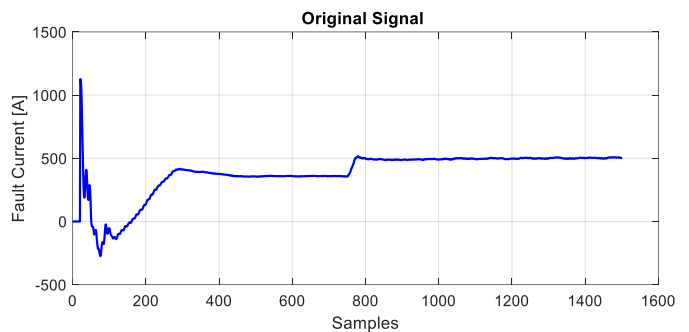


Fig.13. Pole-To-Ground fault, at 10km distance from point M, in the VDC-HVDC system under study

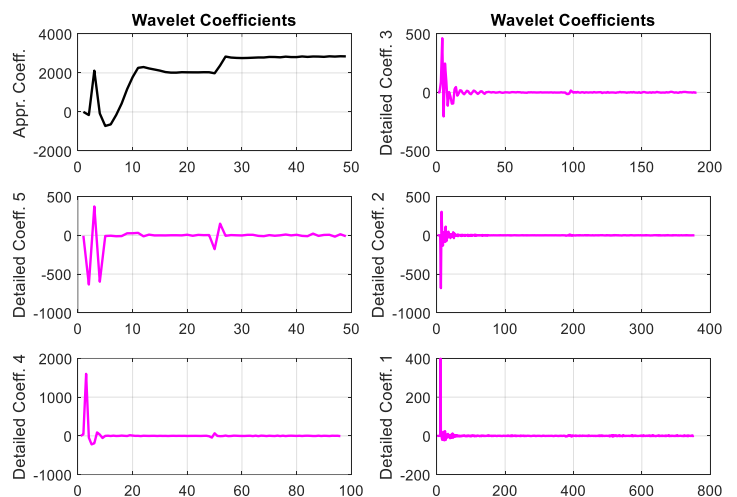


Fig.14.Wavelet coefficients of the pole-to-ground fault current, at 10km distance from point M, in the VSC-HVDC system under study

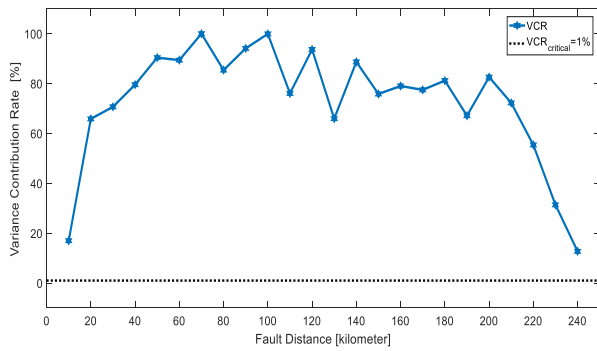


Fig.15. Values of VCR for a pole-to-ground internal fault versus fault distance

4. The Proposed Estimation Model's Performance

To evaluate performance of the proposed estimation model, 24 internal plus 2 external faults are simulated at random distances in MATLAB environment on the VSC-HVDC system. According to Fig.5, upon identification of faults as internal, their effective features will be extracted using DWT technique and then applied as training data to the NSGA-II-based optimized ANFIS. To model the ANFIS's inputs, Gaussian membership functions are assumed. Here, each input feature is described by two parameters, center and width, for all three membership functions. Next, the traditional LS + BP method and the NSGA-II algorithm is applied to determine the optimal values of these parameters. For example, the optimal membership functions using LS+BP and NSGA-II algorithms for one of the ANFIS inputs are plotted in Fig.16. Since there are 9 features for any of the 6 levels, each feature is modeled with 3 membership functions, and each membership function has two parameters, center and width, therefore, there will be a total of 324 parameters to be optimized for ANFIS configuration. The optimal values of center and width parameters for the second feature (standard deviation), for a given PTG fault at a distance of 10 km, are presented in Table (1).

Table (1). Optimal center and width values of three MFs corresponding to the second feature, using different optimization algorithms

Method	NSGA-II	LS+BP
MF 1	[0.0839 0.2392]	[0.0790 0.2062]
MF 2	[0.0954 0.4750]	[0.0886 0.4521]
MF 3	[0.0995 0.6950]	[0.1011 0.7070]

For performance evaluation of the proposed estimation model, 24 internal faults at random distances and 2 external faults are simulated within the system under study and the locations of faults are estimated using the proposed model. The estimation results can be seen in Table (2). To assess the effect of using the extracted features as inputs to ANFIS, two cases are compared against each other. In the first case, samples of the fault current signal are applied to the ANFIS whereas in the second case, signal of the DWT extracted features is used as the ANFIS's input. Also, for each case, the default LS + BP method and NSGA-II algorithm have been used to train the ANFIS. Table (2) demonstrates that by choosing the DWT extracted features as input to the ANFIS, the error is reduced considerably. Using the NSGA-II algorithm for both parameter optimization and ANFIS training also decreases the estimation error. The MSE values for the 4 scenarios under consideration are plotted in Fig.17. For better comparison, in Fig.18, the estimation error is plotted against the fault distance for the four given scenarios. Evidently, the error in the scenario where DWT features are used as the ANFIS's inputs when ANFIS is trained by NSGA-II, is very small. The convergence speed and the final value of the MSE are demonstrated in Figs. 19-21 for 5 repetition of the optimization algorithm.

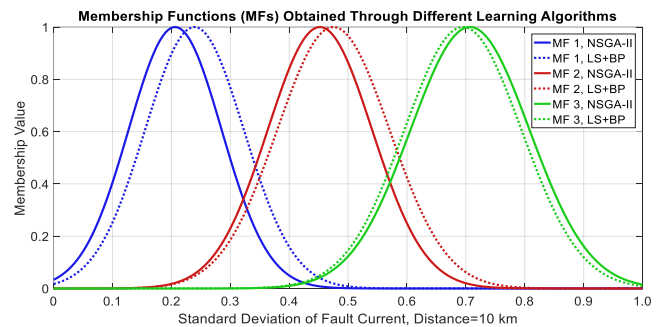


Fig.16. Membership functions of the second feature after optimization by LS+BP method and NSGA-II algorithm

For better comparison, the CDWPSO algorithm used in the previous study [53], is also implemented in this paper for ANFIS training. Comparing the results, it is clear that the NSGA-II optimization algorithm has outstanding performance in terms of convergence speed and final MSE value. This feature is due to the ability of NSGA-II to examine the solutions front simultaneously and escape the local optimality traps. The best numerical value of MSE out of 5 different repetitions for each algorithm is indicated over their corresponding bars (see Fig.17).

Table (2). Performance comparison of the ANFIS-based estimation model for different scenarios

Actual Fault Distance (km)	ANFIS-NSGA-II		ANFIS-LS+BP		VCR (%)
	Features DWT	Current signal	Features DWT	Current signal	
25.6080	25.6413	25.6127	25.6882	26.5625	71.67
54.6720	54.7999	54.7034	54.7702	55.0125	89.37
78.1440	78.1795	78.8203	78.0417	78.6984	87.71
92.0400	92.2849	93.0761	91.4292	92.9413	97.53
115.0800	115.0256	116.1615	114.6783	113.6263	85.91
115.8720	115.6430	114.9010	115.1275	115.2614	88.09
119.5440	119.7463	120.2111	120.4396	118.0036	93.87
126.6480	126.8802	125.7440	127.2086	126.8548	73.54
134.5440	134.3509	134.0147	134.6247	133.0762	73.68
137.9280	138.0545	136.9960	137.0109	139.5752	84.44
140.6400	140.8855	139.5450	140.0599	140.2723	89.20
147.0240	146.8665	147.9248	147.1203	146.0204	80.92
159.9360	160.1158	160.2012	160.2691	160.8261	78.99
167.2080	167.0181	166.0066	168.0898	165.7664	77.51
177.2640	177.4663	176.9020	176.7822	176.3865	81.92
192.3120	192.3857	191.3210	192.2984	191.2238	69.04
195.6960	195.6493	195.7404	196.2961	195.4511	75.30
202.8480	202.8054	204.0628	202.9936	201.8727	82.94
207.6960	207.6122	207.3888	208.3586	208.2659	76.50
210.9600	210.8860	211.6323	210.4566	211.8818	70.72
216.2160	216.2493	216.1474	216.4793	216.8414	62.24
223.1040	223.2841	222.5415	222.2204	222.8223	48.54
232.5360	232.4100	232.2675	233.5017	231.4363	25.42
237.6000	237.7291	237.3791	236.9419	238.2985	15.64
External fault	-	-	-	-	0.9163
Internal fault	-	-	-	-	0.8827
MSE	0.0197	0.4269	0.2445	0.8532	

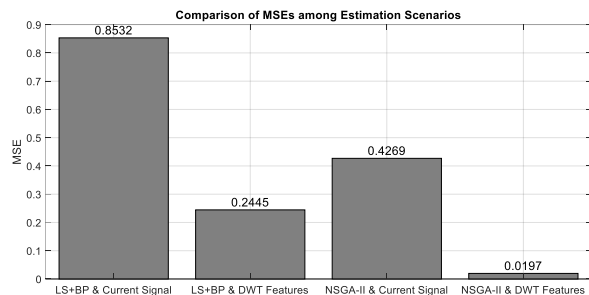


Fig.17. The calculated MSE values for different simulated scenarios

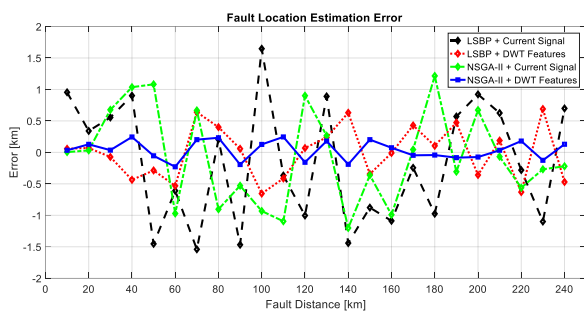


Fig.18. Comparing the estimation errors obtained in different simulated scenarios

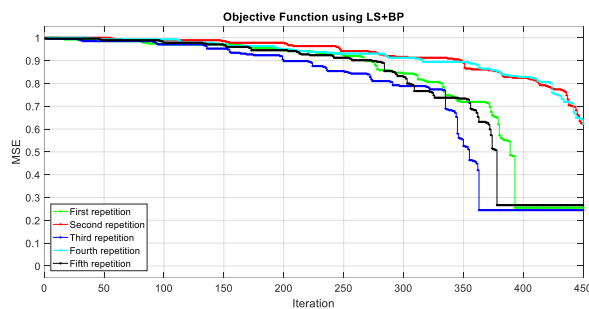


Fig.19. Convergence curve of the LS+BP algorithm for 5 repetitions

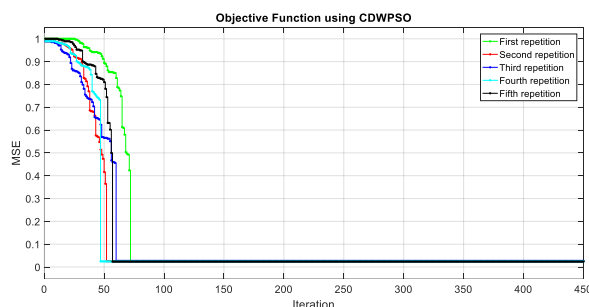


Fig.20. Convergence curve of the CDWPSO algorithm for 5 repetitions

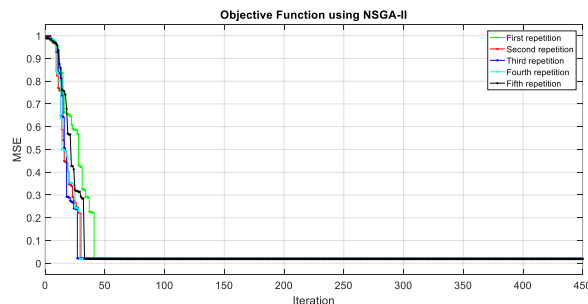


Fig.21. Convergence curve of the NSGA-II algorithm for 5 repetitions

To confirm the performance of NSGA-II algorithm, in addition to the CDWPSO algorithm, the classic PSO and GA algorithms are also simulated the best result during 5 repetitions for each algorithm is shown in Fig.22. From this figure, comparison of results approves the superior performance of the NSGA-II algorithm in terms of convergence speed and estimation accuracy. The parameter of the optimization algorithms are presented in Tables (3)-(6). The statistical results related to the implementation of different optimization algorithms can be seen in Table (7). From this table, it is clear that the proposed NSGA-II algorithm has superior performance compared to other algorithms regarding estimation accuracy and the final value of MSE is also less scattered.

4.1 Comparison with Other Studies

In this section, comparison with other studies in the field has been performed. In [63] and [64], 250 km VSC-HVDC systems has been studied where in both of them, fault location estimation models are proposed. In [63], based on the concept of travelling wave, the natural frequency of the DC line is evaluated. It is found that the natural frequency of the DC line can be influenced by the fault distance and the travelling wave's speed. Furthermore, an integrated method by combining the Fast Fourier Transform (FFT) and PRONY algorithm is proposed in [63] to estimate the dominant natural frequency. The fault current signal is considered as the input; hence, it does not provide the estimation model with effective features, thus, the error percentage is higher. The gap-based method called gap frequency spectrum analysis is proposed in [64]. As in [63], in this method, too, the fault current is used as the input. In order to compare the estimation errors from [63] and [64] with those of this paper, the estimation errors are plotted in Fig.23. In this figure, only five fault distances is considered duo to limitation of the studies performed in [63] and [64]. Also, to carry out a more complete comparison, the estimation error in the previous study [53] was recalculated for the 5 given distances. As can be seen in Fig. 23, the estimation error is much lower using

the proposed ANFIS-NSGA-II + DWT estimation model compared to those of the other methods, especially for more distant faults. The main reason of this characteristic is that

the NSGA-II algorithm can effectively escape the local optimality.

Table (3). Parameters of the GA optimization algorithm

Algorithm	Initial Population	Maximum Iteration	Crossover Method	Crossover Probability	Mutation Probability
Genetic Algorithm	100	450	Two-point method	0.8	0.1

Table (4). Parameters of the PSO optimization algorithm

Algorithm	Number of Particles	Maximum Iteration	Inertia Weight (w)	Cognitive Component (c ₁)	Social Component (c ₂)
Particle Swarm Optimization	100	450	0.5	1.5	1.5

Table (5). Parameters of the CDWPSO optimization algorithm

Algorithm	Initial Population	Maximum Iteration	Inertia Weight (w)	Velocity Limit (k)	Cognitive Component (c ₁)	Social Component (c ₂)
Dynamic Weight Particle Swarm Optimization	100	450	Sine map	0.2	2.0	2.0

Table (6). Parameters of the NSGA-II optimization algorithm

Algorithm	Initial Population	Maximum Iteration	Crossover Probability	Mutation Probability	Distribution index (Crossover)	Distribution index (Mutation)
Non-dominated Sorting Genetic Algorithm II	100	450	0.9	0.1	20	20

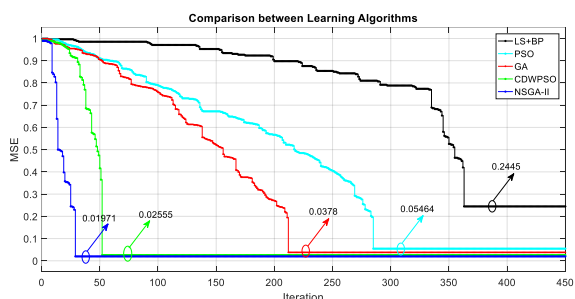


Fig.22. Performance comparison of different optimization algorithms

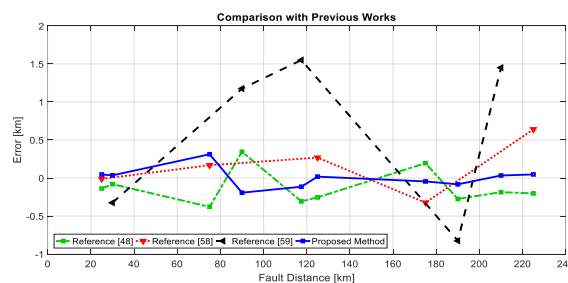


Fig.23. Comparison of estimation error obtained in this work with the literature

Table (7). Performance comparison of different optimization algorithms

Algorithm	Convergence (Iterations)	Standard Deviation	MSE
LS+BP	364	0.5836	0.2445
PSO	285	0.1525	0.0544
GA	212	0.1237	0.0378
CDWPSO	52	0.1106	0.0255
NSGA-II	29	0.0522	0.0197

5. Conclusion

A new fault location estimation method was proposed for a VSC-HVDC system based on ANFIS in this paper, in which the discrete wavelet transform (DWT) scheme has been used to extract effective features. To improve the performance of the ANFIS, the non-dominant sorting genetic algorithm type 2 (NSGA-II) was used for ANFIS training. Using this method, a matrix of useful features was obtained which subsequently was applied as input to ANFIS. The simulation results demonstrate the superiority of the proposed estimation model compared to others in previous studies. The mean square error (MSE) is determined as the objective function which is minimized by optimal training of ANFIS. The ultimate values of MSE by applying different training algorithms, i.e. LS+BP, PSO, GA, CDWPSO, and NSGA-II are compared and the results verify the performance of the proposed model based on the NSGA-II training algorithm. The MSE indicates the estimation error, so the lower this index, the more accurate the estimation model is. In addition, the fast convergence of the proposed NSGA-II helps the system operator to locate the fault source accurately and fast, and isolate the healthy part of the system before severe damage. The accuracy of the proposed model in estimating the fault location is confirmed by comparing the estimation error in the form of a comparative study. The future scope is focused on efforts to evaluate the performance of the proposed model in multi-terminal HVDC system applications and modular multilevel converter (MMC) based HVDC configurations. Since the larger number of signals in these structures, the dimension reduction techniques like principal component analysis (PCA) can be used as integrated feature extraction and selection schemes along with DWT.

References

- [1] V. K. Sood, HVDC and FACTS Controllers, Applications of Static Converters in Power Systems, Kluwer Academic Publishers, 2004.
- [2] D. Jovcic, High Voltage Direct Current Transmission, Converters, Systems and DC Grids, John Wiley & Sons Ltd, 2019.
- [3] N. F. Ibrahim, S. S. Dessouky, Design and Implementation of Voltage Source Converters in HVDC Systems, Springer Nature Switzerland AG, 2021.
- [4] M. Zarif, A. Miranian, "Model predictive control of multi-terminal DC grids with offshore wind farms", International Conference on Renewable Energy Research and Application (ICRERA), 2014, DOI: 10.1109/ICRERA.2014.7016479.
- [5] M. V. Czernorucki, M. B. C. Salles, A. S. Melo, E. C. M da Costa, L. Piegari, "Effects of the HVDC System on converter transformers", International Conference on Renewable Energy Research and Application (ICRERA), 2019, DOI: 10.1109/ICRERA47325.2019.8997095
- [6] C. K. Kim, V. K. Sood, G. S. Jang, S. J. Lim, S. J. Lee, HVDC Transmission: Power Conversion Applications in Power Systems, Wiley-IEEE Press, 2009.
- [7] M. Muniappan, "A comprehensive review of DC fault protection methods in HVDC transmission systems", Protection and Control of Modern Power Systems, DOI: 10.1186/s41601-020-00173-9, Vol. 6, No. 1, January 2021.
- [8] J. P. Keshri, H. Tiwari, "Fault location methods in HVDC transmission system—A review", Intelligent Computing Techniques for Smart Energy Systems. Lecture Notes in Electrical Engineering, Vol. 607, December 2019.
- [9] S. Lan, M. J. Chen, D. Y. Chen, "A novel HVDC double-terminal non-synchronous fault location method based on convolutional neural network", IEEE Trans. on Power Delivery, DOI: 10.1109/TPWRD.2019.2901594, Vol. 34, No. 3, pp. 848-857, June 2019.
- [10] J. Mei et al, "An auxiliary fault identification strategy of flexible HVDC grid based on convolutional neural network with branch structures", IEEE Access, DOI: 10.1109/ACCESS.2020.3004434, Vol. 8, pp. 115922-115931, June 2020.
- [11] N. B. Roy, "Fault identification and determination of its location in a HVDC system based on feature extraction and artificial neural network", Journal of The Institution of Engineers (India): Series B, DOI: 10.1007/s40031-021-00541-5, Vol. 102, No. 2, pp.351-361, April 2021.
- [12] F. M. Aboshady, Mark Sumner, D. W. P. Thomas, "A wideband fault location scheme for active distribution systems", 7th International Conference on Renewable Energy Research and Applications (ICRERA), 2018, DOI: 10.1109/ICRERA.2018.8566780.

- [13] I. A. Gowaid, F. Page, G. P. Adam, B. W. Williams, John Fletcher, "Ring DC node configurations for enhanced DC fault protection in multiterminal HVDC networks", *International Conference on Renewable Energy Research and Applications (ICRERA)*, pp. 1411-1415, 2015, DOI: 10.1109/ICRERA.2015.7418640.
- [14] O. M. K. K. Nanayakkara, A. D. Rajapakse, R. Wachal, "Traveling-wave-based line fault location in star-connected multiterminal HVDC systems", *IEEE Trans. on Power Delivery*, DOI: 10.1109/tpwrd.2012.2202405, Vol. 27, No. 4, pp. 2286-2294, October 2012.
- [15] S. Azizi, M. S. Pasand, M. Abedini, A. Hasani, "A Traveling-Wave-Based Methodology for Wide-Area Fault Location in Multiterminal DC Systems", *IEEE Trans. on Power Delivery*, DOI: 10.1109/TPWRD.2014.2323356, Vol. 29, No. 6, pp. 2552-2560, December 2014.
- [16] L. Yuansheng, W. Gang, L. Haifeng, "Time-domain fault-location method on HVDC transmission lines under unsynchronized two-end measurement and uncertain line parameters", *IEEE Trans. on Power Delivery*, DOI: 10.1109/TPWRD.2014.2335748, Vol. 30, No. 3, pp. 1031-1038, June 2015.
- [17] D. Wang, M. Hou, "Travelling wave fault location principle for hybrid multi-terminal LCC-VSC- HVDC transmission line based on R-ECT", *Electrical Power and Energy Systems*, DOI: 10.1016/j.ijepes.2019.105627, Vol. 117, May 2020.
- [18] H. Cui, N. Tu, "Generalized regression neural networks based HVDC transmission line fault localization", *7th International Conference on Intelligent Human-Machine Systems and Cybernetics*, August 2015.
- [19] L. Zheng, K. Jia, B. Yang, T. Bi, Q. Yang, "Singular value decomposition based pilot protection for transmission lines with converters on both ends", *IEEE Trans. on Power Delivery*, DOI: 10.1109/TPWRD.2021.3115117, pp.1-1, September 2021.
- [20] F. D. Marvasti, A. Mirzaei, "Hybrid travelling wave/distance protection for HVDC transmission lines based on phase angles of characteristic harmonic impedances", *Electrical Engineering*, Vol. 103, pp.2459-2472, March 2021.
- [21] Q. Huai, L. Qin, K. Liu, H. Ding, X. Liao, T. Tan, "Combined line fault location method for MMC-HVDC transmission systems", *IEEE Access*, DOI: 10.1109/ACCESS.2020.3024674, Vol. 8, pp.170794-170804, September 2020.
- [22] Y. Hao, Q. Wang, Y. Li, W. Song, "An intelligent algorithm for fault location on VSC-HVDC system", *International Journal of Electrical Power & Energy Systems*, DOI: 10.1016/j.ijepes.2017.06.030, Vol. 94, pp.116-123, January 2018.
- [23] V. A. Lacerda, R. M. Monaro, D. C. Gaona, D. V. Coury, O. A. Lara, "Distance protection algorithm for multiterminal HVDC systems using the Hilbert-Huang transform", *IET Generation, Transmission and Distribution*, DOI:10.1049/iet-gtd.2019.1551, Vol. 14, No. 15, April 2020.
- [24] L. Xing, Q. Chen, B. Xue, "A fault location method for HVDC transmission lines", *Applied Mechanics and Materials*, Vol. 556-562, pp. 2723-2727, May 2014.
- [25] Y. M. Yeap, N. Geddada, A. Ukil, "Analysis and validation of wavelet transform based DC fault detection in HVDC system", *Applied Soft Computing*, DOI: 10.1016/j.asoc.2017.07.039, Vol. 61, pp. 17-29, December 2017.
- [26] J. Y. Wu, S. Lan, S. J. Xiao, Y. B. Yuan, "Single pole-to-ground fault location system for MMC-HVDC transmission lines based on active pulse and CEEMDAN", *IEEE Access*, DOI: 10.1109/ACCESS.2021.3062703, Vol. 9, pp.42226-42235, February 2021.
- [27] J. M. Johnson, A. Yadav, "Complete protection scheme for fault detection, classification and location estimation in HVDC transmission lines using support vector machines", *IET Science, Measurement & Technology*, DOI: 10.1049/iet-smt.2016.0244, Vol. 11, No. 3, May 2017.
- [28] A. Hadaeghi, H. Samet, T. Ghanbari, "Multi extreme learning machine approach for fault location in multi-terminal high-voltage direct current systems", *Computers & Electrical Engineering*, Vol. 78, pp. 313-327, September 2019.
- [29] M. Farshad, "Locating short-circuit faults in HVDC systems using automatically selected frequency-domain features", *International Trans. on Electrical Energy Systems*, DOI: 10.1002/etep.2765, Vol. 29, No. 3, November 2018.
- [30] H. Wu, Q. Wang, K. Yu, Z. Hu, M. Ran, "A novel intelligent fault identification method based on random forests for HVDC transmission lines", *PLoS ONE*, DOI: 10.1371/journal.pone.0230717, Vol. 15, No. 3, March 2020.
- [31] S. J. Ankar, A. Yadav, "A novel approach to estimate fault location in current source converter-based HVDC transmission line by Gaussian process regression", *International Trans. on Electrical Energy Systems*, DOI: 10.1002/2050-7038.12221, Vol. 30, No. 2, November 2019.
- [32] A. S. Silva, R. C. Santos, J. A. Torres, D. V. Coury, "An accurate method for fault location in HVDC systems based on pattern recognition of DC voltage signals", DOI: 10.1016/j.epsr.2019.01.013, *Electric Power Systems Research*, Vol. 170, pp.64-71, May 2019.
- [33] Shuhui Li, Xingang Fu, Eduardo Alonso, Michael Fairbank, Donald C. Wunsch, "Neural-network based

- vector control of VSCHVDC transmission systems”, International Conference on Renewable Energy Research and Applications (ICRERA), 2015, DOI: 10.1109/ICRERA.2015.7418673.
- [34] N. R. Babu, B. J. Mohan, “Fault classification in power systems using EMD and SVM”, Ain Shams Engineering Journal, DOI: 10.1016/j.asej.2015.08.005, Vol. 8, No. 2, pp. 103-111, June 2017.
- [35] S. Ekici, “Support vector machines for classification and locating faults on transmission lines”, Applied Soft Computing, DOI: 10.1016/j.asoc.2012.02.011, Vol. 12, No. 6, pp. 1650-1658, June 2012.
- [36] A. Prasad, J. B. Edward, K. Ravi, “A review on fault classification methodologies in power transmission systems: Part-II”, Journal of Electrical Systems and Information Technology, DOI: 10.1016/j.jesit.2016.10.003, Vol. 5, No. 1, pp. 61-67, May 2018.
- [37] K. Roy, S. Kar, R. N. Das, Understanding the Basics of QSAR for Applications in Pharmaceutical Sciences and Risk Assessment- Chapter 6: Selected Statistical Methods in QSAR, Elsevier Inc., 2015.
- [38] S. Singh, D. N. Vishwakarma, A. K. Shashank, “A novel methodology for fault detection, classification and location in transmission system based on DWT & ANFIS”, Journal of Information and Optimization Sciences, DOI: 10.1080/02522667.2017.1372129, Vol. 38, No. 6, October 2017.
- [39] S. Barakat, M. B. Eteiba, W. I. Wahba, “Fault location in underground cables using ANFIS nets and discrete wavelet transform”, Journal of Electrical Systems and Information Technology, DOI: 10.1016/j.jesit.2014.12.003, Vol. 1, No. 3, pp. 198-211, December 2014.
- [40] M. Paul, S. Debnath, “ANFIS based single line to ground fault location estimation for transmission lines”, Michael Faraday IET International Summit, DOI: 10.1049/icp.2021.1077, October 2020.
- [41] A. N. Kumar, C. Sanjay, M. Chakravarthy, “Adaptive neuro fuzzy inference system-based fault location technique in double circuit transmission line against simultaneous faults”, Multiscale and Multidisciplinary Modeling, Experiments and Design, DOI: 10.1007/s41939-019-00066-x, Vol. 3, December 2019.
- [42] M. N. M. Salleh, N. Talpur, K. Hussain, “Adaptive neuro-fuzzy inference system: overview, strengths, limitations, and solutions”, International Conference on Data Mining and Big Data, Lecture Notes in Computer Science, Vol. 10387, pp.527-535, June 2017.
- [43] A. Swetapadma, S. Agarwal, A. Ranjan, A. Y. Abdelaziz, “A novel fault distance estimation method for voltage source converter-based HVDC transmission lines”, Electric Power Components and Systems, DOI: 10.1080/15325008.2021.1908447, Vol. 48, No. 16-17, April 2021.
- [44] A. Ghaghishpour, A. Koochaki, “An intelligent method for online voltage stability margin assessment using optimized ANFIS and associated rules technique”, ISA Transactions, DOI: 10.1016/j.isatra.2020.02.028, Vol. 102, pp. 91-104, July 2020.
- [45] K. Paul, P. Dalapati, N. Kumar, “Optimal rescheduling of generators to alleviate congestion in transmission system: A novel modified whale optimization approach”, Arabian Journal for Science and Engineering, Vol. 47, 2022.
- [46] K. Paul, “Modified grey wolf optimization approach for power system transmission line congestion management based on the influence of solar photovoltaic system”, International Journal of Energy and Environmental Engineering, DOI:10.1007/s40095-021-00457-2, Vol. 13, 2022.
- [47] K. Paul, N. Kumar, D. Hati, Anumeha, “Congestion management based on real power rescheduling using moth flame optimization”, Lecture Notes in Electrical Engineering, Vol. 699, Oct. 2020.
- [48] K. Paul, P. Dalapati, “Optimal rescheduling of real power to mitigate congestion using elephant herd optimization”, Lecture Notes in Electrical Engineering, Vol. 702, Jan. 2021.
- [49] K. Paul, N. Kumar, S. Agrawal, “Optimal rescheduling of real power to mitigate congestion with incorporation of wind farm using gravitational search algorithm in deregulated environment”, International Journal of Renewable Energy Research-IJRER, Vol. 7, No. 4, 2017.
- [50] S. Wang, D. Zhao, J. Yuan, H. Li, Y. Gao, “Application of NSGA-II algorithm for fault diagnosis in power system”, Electric Power Systems Research, Vol. 175, October 2019.
- [51] S. Sukumar, S. P. Kar, A. Swain, R. K. Sarangi, P. C. Sekhar, “A combined CFD, ANFIS and NSGA-II model for repetitive pulse laser drilling process”, Lasers in Manufacturing and Materials Processing, Vol. 7, September 2020.
- [52] F. Derbel, N. Derbel and O. Kanoun, Power Systems and Smart Energies, De Gruyter Oldenbourg, 2017.
- [53] R. Rohani, A. Koochaki, “A hybrid method based on optimized neuro-fuzzy system and effective features for fault location in VSC-HVDC systems”, IEEE Access, DOI: 10.1109/ACCESS.2020.2986919, Vol. 8, pp. 70861-70869, April 2020.
- [54] W. Yahui, S. Ling, F. Liuqiang, J. Xiangjie, “NSGA-II algorithm and application for multi-objective flexible workshop scheduling”, Journal of Algorithms & Computational Technology, DOI: 10.1177/1748302620942467, Vol. 14, July 2020.

- [55] N. Huang, G. Lu , G. Cai , D. Xu, J. Xu , F. Li , and L. Zhang, “Feature selection of power quality disturbance signals with an entropy-importance-based random forest”, *Entropy*, DOI: 10.3390/e18020044, Vol. 18, No. 2, January 2016.
- [56] J. B. Ali, N. Fnaiech, L. Saidi, B. C. Morello, F. Fnaiech, “Application of empirical mode decomposition and artificial neural network for automatic bearing fault diagnosis based on vibration signals”, *Applied Acoustics*, DOI: 10.1016/j.apacoust.2014.08.016, Vol. 89, pp. 16-27, March 2015.
- [57] B. Guo, Z. Chen, J. Guo, F. Liu, C. Chen, K. Liu, “Analysis of the nonlinear trends and non-stationary oscillations of regional precipitation in xinjiang, northwestern China, using ensemble empirical mode decomposition”, *International Journal of Environmental Research and Public Health*, DOI: /10.3390/ijerph13030345, Vol. 13, No. 3, March 2016.
- [58] A. F. Güneri, T. Ertay, A. Yücel, “An approach based on ANFIS input selection and modeling for supplier selection problem”, *Expert Systems with Applications*, DOI:10.1016/j.eswa.2011.05.056, Vol. 38, No. 12, pp. 14907-14917, November–December 2011.
- [59] C. A. Coello, G. B. Lamont, D. A. V. Veldhuizen, *Evolutionary Algorithms for Solving Multi-Objective Problems*, Springer Science+Business Media, 2007.
- [60] H. Eristi, O. Yıldırım, B. Eristi, Y. Demir, “Optimal feature selection for classification of the power quality events using wavelet transform and least squares support vector machines”, *International Journal of Electrical Power & Energy Systems*, DOI: 10.1016/j.ijepes.2012.12.018, Vol. 49, pp. 95-103, July 2013.
- [61] A. Ghaghishpour, A. Koochaki, M. Radmehr , “Online Voltage Stability Margin Assessment Using Optimized Adaptive ANFIS and Wavelet Transform Based on Principal Component Analysis”, *Computational Intelligence in Electrical Engineering*, Vol.13, No.22, pp.83-99, 2022.
- [62] S. Hashemi, M. R. Aghamohammadi, “Wavelet based feature extraction of voltage profile for online voltage stability assessment using RBF neural network”, *International Journal of Electrical Power & Energy Systems*, DOI: 10.1016/j.ijepes.2012.12.019, Vol. 49, pp. 86-94, July 2013.
- [63] S. Guobing, C. Xu, C. Xinlei, G. Shuping, R. Mengbing, “A fault-location method for VSC-HVDC transmission lines based on natural frequency of current”, *International Journal of Electrical Power & Energy Systems*, DOI: 10.1016/j.ijepes.2014.05.069, Vol. 63, pp. 347-352, December 2014.
- [64] A Q. Yang, S. L. Blond, B. Cornelusse, P. Vanderbemden, J. Li, “A novel fault detection and fault location method for VSC-HVDC links based on gap frequency spectrum analysis”, *Energy Procedia*, DOI: 10.1016/j.egypro.2017.12.625, Vol. 142, pp. 2243-2249, December 2017.